Autosomal recessive lissencephaly with cerebellar hypoplasia is associated with human *RELN* mutations

Susan E. Hong[1], Yin Yao Shugart[2], David T. Huang[1], Saad Al Shahwan[3], P. Ellen Grant[4], Jonathan O'B. Hourihane[5], Neil D.T. Martin[5] & Christopher A. Walsh[1]

Normal development of the cerebral cortex requires long-range migration of cortical neurons from proliferative regions deep in the brain. Lissencephaly ("smooth brain," from "lissos," meaning smooth, and "encephalos," meaning brain) is a severe developmental disorder in which neuronal migration is impaired, leading to a thickened cerebral cortex whose normally folded contour is simplified and smooth. Two identified lissencephaly genes[1–3] do not account for all known cases[4], and additional lissencephaly syndromes have been described[5]. An autosomal recessive form of lissencephaly (LCH) associated with severe abnormalities of the cerebellum, hippocampus and brainstem maps to chromosome 7q22, and is associated with two independent mutations in the human gene encoding reelin (*RELN*). The mutations disrupt splicing of *RELN* cDNA, resulting in low or undetectable amounts of reelin protein. LCH parallels the reeler mouse mutant (*Reln^rl*), in which *Reln* mutations cause cerebellar hypoplasia, abnormal cerebral cortical neuronal migration and abnormal axonal connectivity[6,7]. *RELN* encodes a large (388 kD) secreted protein[8] that acts on migrating cortical neurons by binding to the very low density lipoprotein receptor (VLDLR), the apolipoprotein E receptor 2 (ApoER2; refs 9–11), α3β1 integrin[12] and protocadherins[13]. Although reelin was previously thought to function exclusively in brain, some humans with *RELN* mutations show abnormal neuromuscular connectivity and congenital lymphoedema, suggesting previously unsuspected functions for reelin in and outside of the brain.

We identified two consanguineous pedigrees with LCH appropriate for linkage analysis. The first (Fig. 1*a*) consisted of British parents who are half-first cousins[14]. At birth, affected children showed normal head size, congenital lymphoedema and hypotonia. Brain magnetic resonance imaging (MRI) showed moderate lissencephaly and profound cerebellar hypoplasia (Fig. 2). Cognitive development was delayed for all affected children, with little or no language and no ability to sit or stand unsupported. There was also myopia, nystagmus and generalized seizures that could be controlled with medication[14]. A second pedigree from Saudi

Arabia (Fig. 1*b*) consisted of a first-cousin marriage with three affected and four unaffected offspring. The affected children showed severe delay in neurological and cognitive development, hypotonia and epilepsy.

Before screening the entire genome for linkage, we tested markers near *RELN* (ref. 15) and *DAB1* (ref. 16), because mutations of the mouse homologues of these two genes cause brain defects in mice that resemble LCH (ref. 7), including hypoplasia of the cerebellum, brainstem abnormalities and a neuronal migration disorder of the neocortex and hippocampus[7,17]. Both pedigrees showed substantial regions of homozygosity (Fig. 1*a,b*) in all affected children near the *RELN* locus in chromosome 7q22, highly suggestive of identity by descent (IBD), whereas neither the clinically normal parents nor any of the normal siblings were homozygous for markers in 7q22. IBD in both pedigrees included a contiguous set of 13 microsatellite markers in 7q22. As expected (given that the two pedigrees are unrelated), there was no evidence of linkage disequilibrium between the two families.

Statistical analysis provided strong evidence for linkage of LCH to chromosome 7q22. Combining the two pedigrees provided a pooled two-point lod score of 3.28 at marker *D7S554* and of 4.02
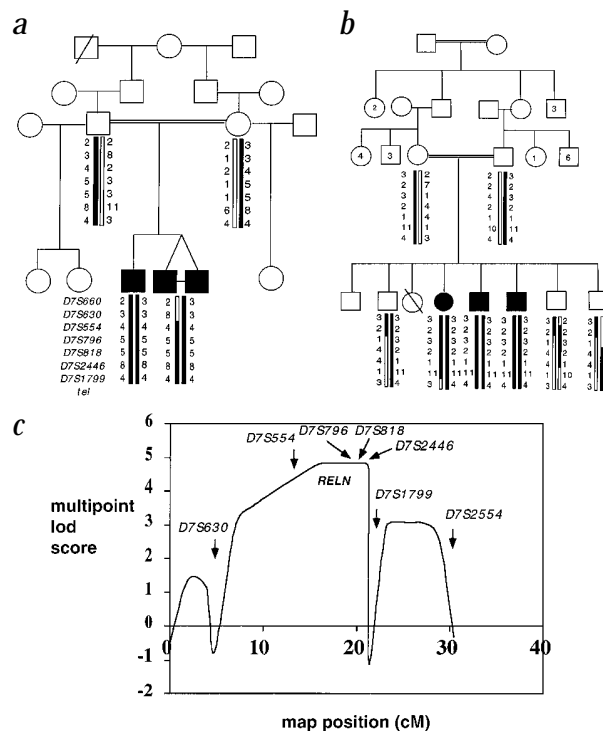
Fig. 1 Pedigree, microsatellite and multipoint linkage analysis of LCH. Pedigrees are illustrated for the British (*a*) and Saudi Arabian (*b*) pedigrees, along with alleles of markers in or near 7q22. Multiple normal siblings who were not tested are indicated by numbers inside of circles or squares. The disease-associated alleles are indicated by shading. Note that all affected individuals are IBD for markers in chromosome 7q22. There is no evidence for linkage disequilibrium between the two pedigrees. Multipoint lod-score analysis of LCH in chromosome 7q22 (*c*) shows relative map positions along the *x* axis and multipoint lod score along the *y* axis. The location of the markers used in the multipoint analysis and the location of *RELN* are indicated. The maximal multipoint lod score is 4.82 in the region of *RELN*. Although the multipoint lod score rises to ~3.0 between 22 and 30 cM, this region is ruled out as a candidate region because of obligatory flanking recombination events.

[1]*Division of Neurogenetics, Department of Neurology, Beth Israel Deaconess Medical Center, Harvard Institutes of Medicine, Boston, Massachusetts, USA.* [2]*Center for Inherited Disease Research, Johns Hopkins University, Bayview Campus, Baltimore, Maryland, USA.* [3]*Departments of Pediatrics and Neuroscience, Riyadh Armed Forces Hospital, Riyadh, Saudi Arabia.* [4]*Neuroradiology Service, Department of Radiology, Massachusetts General Hospital, Boston, Massachusetts, USA.* [5]*Department of Pediatrics, Kent and Canterbury Hospital, Canterbury, Kent, UK. Correspondence should be addressed to C.A.W. (e-mail: cwalsh@caregroup.harvard.edu).*

Fig. 2 MRI analysis of chromosome 7q22-linked lissencephaly with cerebellar hypoplasia (LCH). Standard coronal and parasagittal views are shown from a normal individual (*a*,*b*), an affected member of the British pedigree (*c*,*d*) and an affected member of the Saudi Arabian pedigree (*e*,*f*). Axial views of the cortex (*g*) and pons (*h*) from other members of the Saudi Arabian pedigree are also shown. The cortex is thickened and the gyral pattern is simplified (*c*–*f*). Both of these abnormalities are more severe frontally and temporally, so that the thickness and gyral pattern of the occipital and parietal cortex are relatively normal (*c*,*e*,*g*). The hippocampus (asterisk) fails to undergo its normal pattern of infolding, and consequently appears flattened, lacking definable upper and lower blades (*f*). The subcortical white matter is decreased in amount but consistently normal in its signal characteristics. The corpus callosum is thin but present over its entire rostral-caudal extent (*c*,*e*). The lateral ventricles are enlarged, which is a common finding in congenital brain abnormalities, representing persistence of the fetal ventricular configuration rather than true hydrocephalus. The cerebellum (arrow in *c*) is severely reduced in size (*c*,*e*), with hypoplasia of the inferior vermis and cerebellar hemispheres, devoid of any detectable folia (folds) or normal architecture. The pons (arrowhead in *e*) is reduced in size in superior-inferior and antero-posterior extent (*c*,*e*,*h*). The normal ventral bulge of the pons, formed by fibres of the middle cerebellar peduncles, is greatly reduced in size, commensurate with the hypoplasia of the cerebellum (*c*,*e*,*h*). All visualized cranial nerves appeared normal, including II, III, V, VII, VIII and XII (*b*,*d*,*f*).
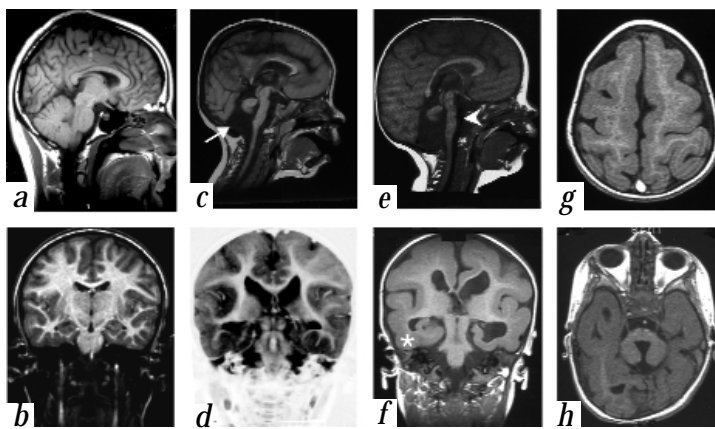
at *D7S2446* (Table 1). Nonparametric linkage analysis also provided highly significant evidence for linkage of LCH to 7q22 ($P < 0.00003$). Multipoint analysis provided a maximal lod score greater than 4.8 (Fig. 1*c*). These data and analysis of homozygosity indicated a minimal candidate interval for LCH of approximately 15 cM between *D7S630* and *D7S1799*. Because *RELN* is contained within this interval, we tested it for mutations in LCH.

Reelin is encoded by 65 exons, covering more than 400 kb of genomic DNA and 12 kb of coding cDNA (refs 7,15,18). We amplified the entire *RELN* cDNA using nested RT–PCR amplification of RNA from immortalized lymphoblastoid cell lines, and detected a normal, previously described[7,18,19] splice variant that removed 6 bp of coding sequence (exon 63) without altering the reading frame. In affected individuals in the Saudi Arabian pedigree, the remainder of the RT–PCR products were normal except between nt 5,123 and 6,189, where RT–PCR products were 85 bp shorter than normal in affected patients only (Fig. 3*a*,*b*). DNA sequence analysis of the aberrant PCR product revealed normal sequence until bp 5,705 of the ORF, corresponding to the end of exon 35, and normal sequence corresponding to the beginning of exon 37, but precise deletion of 85 bp corresponding to exon 36 (Fig. 3*b*). The apposition of exon 35 to exon 37 indicates abnormal splicing, which deletes exon 36 and produces a translational frameshift with the addition of 22 missense amino acids, followed by a premature termination codon.

Sequence analysis of genomic DNA from affected patients (Fig. 3*c*) revealed a mutation at the splice acceptor sequence of exon 36 that changes the sequence from CAG to CAA. There is a G at position –1 bp in 100% of known splice-acceptor sites[20]. All three affected patients in this family were homozygous for the splice-acceptor mutation (Fig. 3*c*, and data not shown). The parents were both heterozygous for the mutant CAA sequence and the normal CAG sequence (Fig. 3*d*,*e*). The DNA sequence of 90 normal individuals (45 European and 45 Saudi Arabian or other Middle Eastern Arabic individuals) showed homozygosity for the normal CAG sequence in all samples (Fig. 3*f*).

We identified a second distinct mutation in the British pedigree. RT–PCR products were once again normal in size and sequence except between nt 6,696 and 6,844 (Fig. 3*g*). We observed several abnormal PCR products, including a predominant PCR product approximately 150 bp shorter than normal (Fig. 3*g*). Sequence analysis of the aberrant RT–PCR product indicated that it matched the *RELN* cDNA sequence until bp 6,696, corresponding to the end of exon 41, and after bp 6,844, the beginning of exon 43. The removal of exon 42 in the mutant cDNA deletes 148 bp (Fig. 3*g*,*h*), producing a translational frameshift and early termination codon following 6 missense amino acids. DNA sequence analysis of

genomic DNA between exons 41 and 43 in affected patients did not reveal gross rearrangements or mutations at the most highly conserved splice donor and acceptor sequences, although other mutations in these introns or elsewhere could not be excluded.

To confirm that the splicing mutations affect reelin protein, we analysed serum from both pedigrees, as reelin has recently been detected in normal human serum[21]. Reelin is present in serum as three bands of approximately 420 kD, 310 kD and 160 kD, which seem to represent proteins with post-translational modifications (Fig. 4*a*,*b*). In the Saudi Arabian pedigree, reelin was undetectable in affected patients, whereas parents and unaffected siblings

Table 1 • Two-point lod score table for mapping of LCH to markers in chromosome 7q22

Marker	θ	0.0	0.01	0.05	0.1	0.2	0.3	0.4
D7S660								
Zmax total		−0.44	−0.04	0.45	0.61	0.53	0.29	0.07
Ped2		0.84	0.87	0.90	0.84	0.61	0.32	0.08
Ped1		−1.28	−0.92	−0.45	−0.24	−0.08	−0.03	−0.01
D7S630								
Zmax total		−1.98	−0.01	0.52	0.62	0.52	0.33	0.14
Ped2		0.75	0.74	0.67	0.58	0.40	0.24	0.10
Ped1		−2.73	−0.75	−0.14	0.04	0.12	0.09	0.04
D7S554								
Zmax total		3.28	3.20	2.89	2.50	1.71	0.97	0.35
Ped2		2.13	2.09	1.90	1.66	1.18	0.70	0.27
Ped1		1.14	1.11	0.99	0.84	0.54	0.27	0.08
D7S796								
Zmax total		2.77	2.71	2.45	2.12	1.47	0.86	0.34
Ped2		1.49	1.46	1.33	1.16	0.83	0.51	0.22
Ped1		1.28	1.25	1.12	0.96	0.64	0.35	0.12
D7S818								
Zmax total		2.77	2.71	2.45	2.12	1.47	0.86	0.34
Ped2		1.49	1.46	1.33	1.16	0.83	0.51	0.22
Ped1		1.28	1.25	1.12	0.96	0.64	0.35	0.12
D7S2446								
Zmax total		4.02	3.94	3.60	3.17	2.30	1.44	0.50
Ped2		2.64	2.59	2.38	2.12	1.58	1.03	0.50
Ped1		1.38	1.35	1.22	1.05	0.72	0.40	0.15
D7S1799								
Zmax total		−2.65	0.23	0.73	0.79	0.62	0.38	0.16
Ped2		−3.49	−0.59	−0.00	0.16	0.20	0.14	0.07
Ped1		0.84	0.82	0.74	0.63	0.42	0.23	0.09
D7S2554								
Zmax total		−0.77	−0.11	0.33	0.39	0.24	0.04	−0.04
Ped2		−1.4	−0.78	−0.22	−0.02	0.09	0.07	0.02
Ped1		0.70	0.67	0.56	0.42	0.15	−0.03	−0.06

Markers are ordered from centromere (top) towards the telomere. The marker order is taken from the Whitehead map. Ped1 refers to the British pedigree, and Ped2 to the Saudi Arabian pedigree.
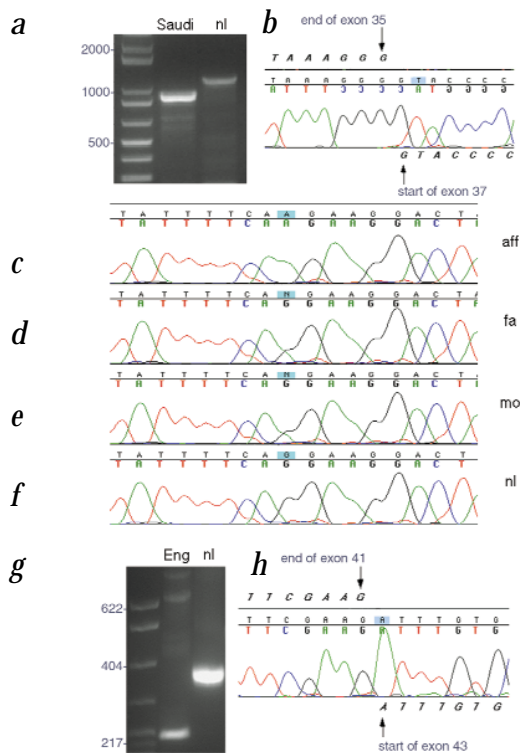
Fig. 3 Mutational analysis of *RELN* in LCH. *a*, Agarose gel electrophoresis of an RT–PCR product from an affected child in the Saudi Arabian pedigree (Saudi) compared with normal (nl), using primers spanning nt 5,123–6,189 of the coding sequence. The resulting PCR product is 85 bp smaller than normal. *b*, DNA sequence analysis of the abnormal PCR product (*a*), which is normal in sequence up to the end of exon 35, and normal again after the beginning of exon 37, indicating a splicing abnormality that deletes exon 36. Sequence analysis of genomic DNA from an affected (aff) patient (*c*) shows that patients are homozygous for a mutation that changes the splice acceptor from CAG to CAA, altering the G that is present in 100% of known splice acceptor sites[20]. Other affected patients in this family were also homozygous for this mutation (not shown). The parents (fa, mo) were both heterozygous for the mutation (*d,e*), and the sequence of a normal control (nl) is shown in (*f*). *g*, An RT–PCR product of a segment of *RELN* cDNA from a normal (nl) and an affected patient from the British pedigree (Eng), illustrating the shortened PCR product present in the patient sample, which is 148 bp shorter than normal due to skipping of exon 42. The mutant sequence is normal up to bp 6696 of the cDNA sequence, at the end of exon 41, and at bp 6844 of the cDNA, indicating a deletion of the cDNA of 148 bp, corresponding to a skipping of exon 42.

showed normal or reduced levels of the three reelin bands, consistent with the heterozygous state (Fig. 4*a*). In affected patients in the British pedigree, reelin levels were reduced in affected patients and were only barely detectable if samples were deliberately overloaded on the gel (Fig. 4*b*). Because the affected children in both pedigrees are clinically and radiographically indistinguishable, we conclude that both mutations are probably null alleles.

The two human splicing mutations in *RELN* resemble naturally occurring mouse *Reln^rl* alleles. The Saudi Arabian mutation truncates the predicted protein after the fourth reelin repeat (Fig. 5*a,b*), deleting 1,616 amino acids and the highly basic carboxy terminus that is required for normal secretion and function[22,23]. The British mutation truncates the predicted protein in the fifth repeat, removing 1,229 amino acids (Fig. 5*a,b*) including the highly basic C terminus. Both human mutations resemble the *Reln^rl-Alb2* allele (Fig. 5*c*), in which a retrotransposon insertion into exon 37 causes skipping of that exon with a translational frameshift[24]. In a second naturally occurring mouse allele, *Reln^rl-Orl* (Fig. 5*c*), an L1 element inserted into exon 61 produces skipping of that exon with a translational frameshift[23,25,26]. The *Reln^rl-Orl* and *Reln^rl-Alb2* alleles are phenotypically indistinguishable from alleles in which reelin protein is undetectable.

Fig. 4 Western-blot analysis shows loss of reelin from the serum of LCH patients. *a*, Western-blot analysis of serum from a normal control (nl serum) and from the father, normal siblings (nl sib 1, nl sib 2), mother and two affected children with LCH in the Saudi Arabian family. Reelin is normally present in serum as three bands at ~420, 310 and 160 kD (arrows; ref. 21), which appear to represent post-translational modifications of the protein, as they are all present when *RELN* cDNA is transfected into cultured cells (rln sup). Parents (heterozygous for mutations) and unaffected siblings show preserved reelin immunoreactivity, with occasional decreased amounts consistent with the heterozygous state. Both affected offspring show no detectable reelin, even when the lanes are overloaded and overexposed. Loading controls indicate a band of comparable size from the Ponceau staining of the original gel. *b*, Western-blot analysis of serum from normal controls and from the parents and three affected offspring of the British pedigree. Parents show preserved reelin immunoreactivity, whereas all three affected patients (affected 1, affected 2, affected 3) show reduction of reelin staining, with bands being faintly detectable only when samples from affected individuals are deliberately overloaded. The location of a size standard (187 kD) is indicated.

Whereas the phenotype effected by human *RELN* mutations resembles the *Reln^rl* mouse (Fig. 2), human LCH patients point to several previously unsuspected functions of reelin in and outside the brain. Although abnormalities of *RELN* mRNA have been reported in postmortem brains of schizophrenic humans[27], we found no evidence of schizophrenia in individuals with heterozygous or homozygous *RELN* mutations. On the other hand, the one LCH patient studied with a muscle biopsy showed evidence of abnormal neuromuscular connectivity[14]. Moreover, at least three patients had persistent lymphoedema neonatally, and one showed accumulation of chlyous (that is, fatty) ascites fluid that required peritoneal shunting[14]. The apparent role for reelin in serum homeostasis may reflect reelin interactions with LDL superfamily receptors outside the brain, as well as in the brain.
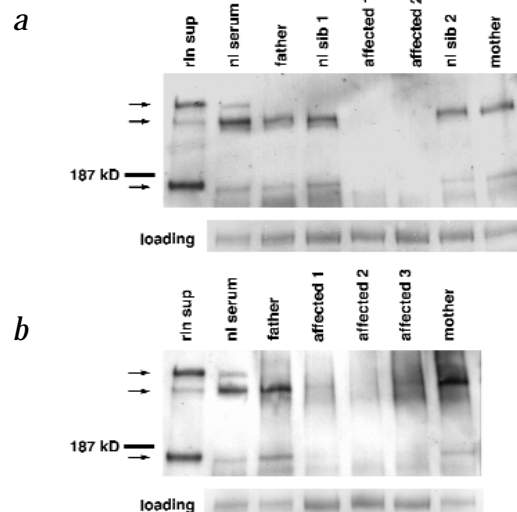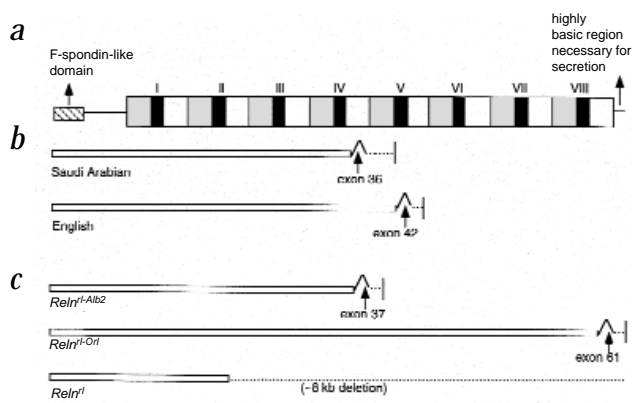
Methods

Patient ascertainment. We enrolled patients after obtaining informed consent in accordance with protocols approved by the Institutional Review Board of Beth Israel Deaconess Medical Center. MRI imaging was performed at several sites and used standard clinical protocols. Peripheral blood obtained by antecubital venipuncture was subjected to lymphocyte separation using Lymphocyte Separation Medium (Organon Technica). We used kits (Qiagen) to prepare DNA from lymphocytes using standard techniques. The Genomics Core Facility at Massachusetts General Hospital created immortalized lymphoblastoid cell lines from selected patients using standard techniques of Epstein-Barr virus-mediated transformation.

Fig. 5 Effects of human and naturally occurring mouse *RELN* mutations on the predicted protein. ***a***, The predicted reelin protein. It consists of a region of homology to F-spondin at the amino terminus, followed by 8 'reelin' repeats, each consisting of an internal EGF-like repeat flanked by reelin-specific sequence. The C terminus includes many highly charged amino acids that appear to be required for secretion. ***b***, Schematic views of the Saudi Arabian and British mutant alleles. The Saudi Arabian allele causes skipping of exon 36, which causes a translational frameshift and early termination codon following the addition of 22 missense amino acids. The British mutation skips exon 42, which also creates a termination codon in the middle of the fifth reelin repeat, after the addition of 6 missense amino acids. ***c***, All known naturally occurring mouse mutant alleles of *Reln* (ref. 7). Two of the three known alleles are splicing mutations similar to the human alleles. The *Reln^rl-Alb2* allele skips exon 37 and the *Reln^rl-Orl* allele skips exon 61, and both of these alleles appear to be complete null alleles.

Microsatellite analysis. We identified appropriate microsatellite markers from published[15] and the Marshfield (http://www.marshmed.org/genetics/) and Genethon maps[28], purchased them as PCR primers (Research Genetics) and amplified them from patient DNA samples using standard conditions. We separated the PCR products on denaturing polyacrylamide gels, visualized the products using silver staining (Promega) and determined alleles by running size standards. The allele sizes and frequencies are from the Genome Database (http://gdbwww.gdb.org/) and Marshfield web sites.

Linkage analysis. We performed parametric and nonparametric analyses using the Genehunter program, considering the twins in the British pedigree to be monozygotic. For the parametric analyses, we assumed a susceptibility allele with frequency 0.01 and penetrance of 0.9. We performed multipoint analyses for *D7S630*, *D7S554*, *D7S796*, *D7S818*, *D7S2446*, *D7S1799* and *D7S2554*. Allele frequencies for *D7S554*, *D7S818* and *D7S1799* were not available and therefore were assumed to be equal. However, the influence of allele frequencies on the multipoint results was examined. We changed the allele frequencies from the most prevalent alleles to different values and the results did not change significantly. Nonparametric tests for linkage were also performed in which we did not have to specify any genetic parameters such as penetrance and disease allele frequency.

Mutation analysis. We designed RT–PCR primers using Oligo and Primer3 (http://www.embnet.sk/cgi-bin/primer3/primer3_www.cgi). Initial PCR reactions (35 cycles) generally spanned 1–1.2 kb of *RELN* cDNA, with secondary, hemi-nested PCR reactions (35 cycles) consisting of fragments 400–600 bp in length suitable for direct DNA sequencing. Sequences of PCR primers are available on request. DNA sequence analysis was performed using the dye termination reaction and Big Dyes (Perkin Elmer). We separated and read the sequence products on an ABI377 automated sequencer, and contiged and analysed them using the Sequencher (Genecodes) program.

Western-blot analysis. Serum (1 μl) diluted into denaturing sample buffer was run on 4–15% gradient gels (Biorad) and transferred overnight onto Immobilon-P membranes (Millipore). We stained the blots with Ponceau to normalize loading, then blocked them in 4% nonfat dry milk (1 h) and incubated them overnight in anti-reelin (142) antiserum at 1:200 dilution. We then rinsed the blots, incubated them in HRP-conjugated goat anti-mouse IgG secondary antibody at 1:2,000 for 1 h, rinsed them again, then incubated them in LumiGlo Chemiluminescent Substrate (KPL) for 1 min and exposed them to film (X-OMAT LS, Kodak) for 2–45 min.

1. Reiner, O. *et al.* Isolation of a Miller-Dieker lissencephaly gene containing G protein β-subunit-like repeats. *Nature* **364**, 717–721 (1993).
2. Gleeson, J.G. *et al.* Doublecortin, a brain-specific gene mutated in human X-linked lissencephaly and double cortex syndrome, encodes a putative signaling protein. *Cell* **92**, 63–72 (1998).
3. des Portes, V. *et al.* A novel CNS gene required for neuronal migration and involved in X-linked subcortical laminar heterotopia and lissencephaly syndrome. *Cell* **92**, 51–61 (1998).
4. Pilz, D.T. *et al.* LIS1 and XLIS (DCX) mutations cause most classical lissencephaly, but different patterns of malformation. *Hum. Mol. Genet.* **7**, 2029–2037 (1998).
5. Walsh, C.A. Genetic malformations of the human cerebral cortex. *Neuron* **23**, 19–29 (1999).
6. Caviness, V.S. & Rakic, P. Mechanisms of cortical development: a view from mutations in mice. *Annu. Rev. Neurosci.* **1**, 297–326 (1978).
7. Lambert de Rouvroit, C. & Goffinet, A.M. The reeler mouse as a model of brain development. *Adv. Anat. Embryol. Cell Biol.* **150**, 1–106 (1998).
8. D'Arcangelo, G. *et al.* A protein related to extracellular matrix proteins deleted in the mouse mutant reeler. *Nature* **374**, 719–723 (1995).
9. D'Arcangelo, G. *et al.* Reelin is a ligand for lipoprotein receptors. *Neuron* **24**, 471–479 (1999).
10. Hiesberger, T. *et al.* Direct binding of Reelin to VLDL receptor and ApoE receptor 2 induces tyrosine phosphorylation of disabled-1 and modulates tau phosphorylation. *Neuron* **24**, 481–489 (1999).
11. Trommsdorff, M. *et al.* Reeler/Disabled-like disruption of neuronal migration in knockout mice lacking the VLDL receptor and ApoE receptor 2. *Cell* **97**, 689–701 (1999).
12. Dulabon, L. *et al.* Reelin binds α3β1 integrin and inhibits neuronal migration. *Neuron* **27**, 33–44 (2000).
13. Senzaki, K., Ogawa, M. & Yagi, T. Proteins of the CNR family are multiple receptors for Reelin. *Cell* **99**, 635–647 (1999).
14. Hourihane, J.O., Bennett, C.P., Chaudhuri, R., Robb, S.A. & Martin, N.D.T. A sibship with a neuronal migration defect, cerebellar hypoplasia and congenital lymphedema. *Neuropediatrics* **24**, 43–46 (1993).
15. DeSilva, U. *et al.* The human reelin gene: isolation, sequencing, and mapping on chromosome 7. *Genome Res.* **7**, 157–164 (1997).
16. Lambert de Rouvroit, C. & Goffinet, A.M. Cloning of human DAB1 and mapping to chromosome 1p31–p32. *Genomics* **53**, 246–247 (1998).
17. Gonzalez, J.L. *et al.* Birthdate and cell marker analysis of scrambler: a novel mutation affecting cortical development with a reeler-like phenotype. *J. Neurosci.* **17**, 9204–9211 (1997).
18. Royaux, I., Lambert de Rouvroit, C., D'Arcangelo, G., Demirov, D. & Goffinet, A.M. Genomic organization of the mouse reelin gene. *Genomics* **46**, 240–250 (1997).
19. Lambert de Rouvroit, C., Bernier, B., Royaux, I., de Bergeyck, V. & Goffinet, A.M. Evolutionarily conserved, alternative splicing of reelin during brain development. *Exp. Neurol.* **156**, 229–238 (1999).
20. Shapiro, M.B. & Senapathy, P. RNA splice junctions of different classes of eukaryotes: sequence statistics and functional implications in gene expression. *Nucleic Acids Res.* **15**, 7155–7174 (1987).
21. Smalheiser, N.R. *et al.* Expression of reelin in adult mammalian blood, liver, pituitary pars intermedia, and adrenal chromaffin cells. *Proc. Natl Acad. Sci. USA* **97**, 1281–1286 (2000).
22. D'Arcangelo, G. *et al.* Reelin is a secreted glycoprotein recognized by the CR-50 monoclonal antibody. *J. Neurosci.* **17**, 23–31 (1997).
23. de Bergeyck, V. *et al.* A truncated Reelin protein is produced but not secreted in the 'Orleans' reeler mutation (Reln[rl-Orl]). *Brain Res. Mol. Brain Res.* **50**, 85–90 (1997).
24. Royaux, I., Bernier, B., Montgomery, J.C., Flaherty, L. & Goffinet, A.M. Reln(rl-Alb2), an allele of reeler isolated from a chlorambucil screen, is due to an IAP insertion with exon skipping. *Genomics* **42**, 479–482 (1997).
25. Takahara, T. *et al.* Dysfunction of the orleans reeler gene arising from exon skipping due to transposition of a full-length copy of an active L1 sequence into the skipped exon. *Hum. Mol. Genet.* **5**, 989–993 (1996).
26. Hirotsune, S. *et al.* The reeler gene encodes a protein with an EGF-like motif expressed by pioneer neurons. *Nature Genet.* **10**, 77–83 (1995).
27. Impagnatiello, F. *et al.* A decrease of reelin expression as a putative vulnerability factor in schizophrenia. *Proc. Natl Acad. Sci. USA* **95**, 15718–15723 (1998).
28. NIH/CEPH Collaborative Mapping Group A comprehensive genetic linkage map of the human genome. *Science* **258**, 67–86 (1992).